ATTACHMENT 4

CDI REPORT NO. 10-09NP, "ACM REV. 4.1: METHODOLOGY TO PREDICT FULL SCALE STEAM DRYER LOADS FROM IN-PLANT MEASUREMENTS," REV. 1 (NON-PROPRIETARY)

Nine Mile Point Nuclear Station, LLC
June 30, 2010

This Document Does Not Contain Continuum Dynamics, Inc. Proprietary Information

C.D.I. Report No. 10-09NP

ACM Rev. 4.1: Methodology to Predict Full Scale Steam Dryer Loads from In-Plant Measurements

Revision 1

Prepared by

Continuum Dynamics, Inc.
34 Lexington Avenue
Ewing, NJ 08618

Prepared by

Milton E. Teske

Approved by

Alan J. Bilanin

June 2010

Executive Summary

Measured in-plant pressure time-history data in the four main steam lines of Quad Cities Unit 2 (QC2), inferred from strain gage data collected at two positions upstream of the ERV standpipes on each of the main steam lines, are used with Continuum Dynamics, Inc.'s acoustic circuit model of the QC2 steam dome and steam lines to predict steam dryer loads. The strain gage data are first converted to pressures, and are then used to extract acoustic sources in the system. Once these sources are obtained, the model is used to predict the pressure time histories at locations on the steam dryer where pressure sensors were positioned. These predictions are then compared against data from the pressure sensors, and model bias and uncertainty are evaluated.

These results provide a revised model that bounds the pressure loads on a steam dryer, and thereby enables the dryer to be analyzed structurally for its fitness during power ascension and EPU operations.

Table of Contents

Section		Page
	Executive Summary	i
	Table of Contents	ii
1.	Introduction	1
2.	Overview of Methodology	3
	2.1 Helmholtz Analysis	3
	2.2 Acoustic Circuit Analysis	3
	2.3 Low Frequency Contribution	4
	2.4 Modeling Parameters	4
	2.5 Model Assembly and Algorithm	5
	2.6 Pressure Location Solution	6
3.	Quad Cities Unit 2 Instrumentation and Plant Data	8
4.	Low Frequency Hydrodynamic Load Contribution	9
5.	Noise Reduction in Measured Main Steam Line Data	11
	5.1 Coherence Filtering	11
	5.2 Corrected Coherence Values	12
	5.3 Application to QC2 Data	13
6.	Model Predictions and Comparisons	23
7.	Model Uncertainty	33
8.	Application to QC2 Steam Dryer	35
9.	Conclusions	42
10.	References	43

1. Introduction

In the spring of 2005, Exelon Generation LLC installed new steam dryers into its Quad Cities Unit 2 (QC2) and Quad Cities Unit 1 nuclear power plants. The replacement design, developed by General Electric, sought to improve dryer performance and overcome structural inadequacies identified on the original dryers. The design had been previously analyzed by extrapolating acoustic circuit model predictions from the original dryer to produce expected full-scale vulnerability loads [1] and from modeling the new dryer in the SMT (subscale model test) to produce corresponding loads from subscale data [2]. The QC2 dryer was instrumented with pressure sensors at 27 locations, and these data could be used to validate the acoustic circuit model. These pressure data formed the set of data to be first predicted (blind evaluation) and then corrected (modified evalution) utilizing only data measured on the main steam lines. Data collection was undertaken at 790 MWe (2493 MWt), just short of Original Licensed Thermal Power (OLTP) conditions, and at 930 MWe (2885 MWt), near Extended Power Uprate (EPU) conditions. At QC2, OLTP is rated at 2511 MWt, while EPU is rated at 2957 MWt.

Scaling analysis has shown that the unsteady pressure P′ must scale as

$$\frac{P'}{\frac{1}{2}\rho U^2} = \text{fcn}\left(M = \frac{U}{a}, \text{Re} = \frac{\rho U D}{\mu}, \frac{L_1}{L}, \frac{L_2}{L}, \ldots \right) \tag{1.1}$$

where M is the Mach number, Re is the Reynolds number, U is the main steam line flow speed, a is the acoustic speed, ρ is the fluid density, D is the diameter of the main steam line, μ is the fluid viscosity, and L, L_1, L_2, … are lengths. Tabulation of the EPU Mach numbers for plants seeking EPU licenses are shown in Table 1.1, and show that the QC2 790 MWe data (at OLTP conditions) have a Mach number representative of these plants and that this dataset is the appropriate one to examine.

The overall results, encompassing (1) a blind evaluation at 790 MWe, (2) a modified evaluation at 790 MWe, (3) a blind evaluation at 930 MWe, (4) a modified evaluation at 930 MWe, (5) a pressure sensor evaluation at 930 MWe, and (6) a strain gage and pressure sensor evaluation at 930 MWe, are described in [3]. A later blind evaluation at 912 MWe (2831 MWt) and an evaluation at 842 MWe (2493 MWt) are described in [4]. The accuracy of these model predictions was judged by model agreement with data at six of the pressure sensors mounted on the steam dryer. Following further review, it became clear that, although model evaluations (4) and (6) tracked the data well for most pressure sensors, the data from several of the pressure sensors were under-predicted in the critical frequency range of 145 Hz to 165 Hz. Thus, Exelon requested that model parameters be re-examined to see whether a better comparison with the pressure sensor data could be achieved. That effort resulted in a model that matched the mean of the root mean square (RMS) of the pressure data at the 27 sensors on the QC2 dryer [5].

Later work (reported in [6]) developed acoustic circuit model parameters which resulted in dryer pressure load predictions on the outer bank hoods of the steam dryer that bounded the

pressure loads measured there, and therefore provided steam dryer load predictions more conservative than those reported previously. [[

(3)]]

Table 1.1. Estimated EPU Mach numbers for plants seeking EPU license.

Plant	EPU Mach Number
Browns Ferry	0.100
Hope Creek	0.105
Monticello	0.113
Laguna Verde	0.111
Nine Mile Point	0.110
Susquehanna	0.100
Vermont Yankee	0.109

Plant	OLTP Mach Number
Quad Cities Unit 2	0.105

2. Overview of Methodology

The QC2 steam supply system is divided into two distinct analyses: a Helmholtz solution within the steam dome and an acoustic circuit analysis in the main steam lines. This section of the report highlights the two approaches taken here. All analyses are undertaken in frequency space and the pressure P used here is the Fourier transformed pressure.

2.1 Helmholtz Analysis

The three-dimensional geometry of a steam dome and steam dryer is rendered onto a uniformly-spaced rectangular grid, and a solution is obtained for the Helmholtz equation

$$\frac{\partial^2 P}{\partial x^2}+\frac{\partial^2 P}{\partial y^2}+\frac{\partial^2 P}{\partial z^2}+\frac{\omega^2}{a^2}P=\nabla^2 P+\frac{\omega^2}{a^2}P=0 \tag{2.1}$$

where P is the pressure at a grid point, ω is frequency, and a is complex acoustic speed. This equation is solved at 5 Hz increments from 0 to 250 Hz, subject to the boundary conditions

$$\frac{dP}{dn}=0 \tag{2.2}$$

normal to all solid surfaces (the steam dome wall and interior and exterior surfaces of the dryer),

$$\frac{dP}{dn}=\frac{i\omega Z}{a}P \tag{2.3}$$

normal to the nominal water level surface, and unit pressure applied to one inlet to a main steam line and zero applied to the other three. In all of the equations presented here, $i=\sqrt{-1}$, and time dependence of the form $e^{i\omega t}$ is implied. The Helmholtz solutions have been shown to vary slowly between the 5 Hz increments chosen here [8].

2.2 Acoustic Circuit Analysis

The Helmholtz solution within the steam dome is coupled to an acoustic circuit solution in the main steam lines. Pulsation in a single-phase compressible medium, where acoustic wavelengths are long compared to component dimensions, and in particular long compared to transverse dimensions (directions perpendicular to the primary flow directions), lend themselves to application of the acoustic circuit methodology. If the analysis is restricted to frequencies below 250 Hz, acoustic wavelengths are approximately six feet in length, and wavelengths are therefore long compared to most components of interest, such as branch junctions.

Acoustic circuit analysis divides the main steam lines into elements, which are each characterized by a length L, a cross-sectional area A, a fluid mean density ρ, a fluid mean flow velocity $\overline{U}$, and a fluid acoustic speed a.

Application of the acoustic circuit methodology generates solutions for the fluctuating pressure P_n and velocity u_n in the nth element of the form

$$P_n = \left[A_n e^{ik_{1n}X_n} + B_n e^{ik_{2n}X_n}\right] e^{i\omega t} \tag{2.4}$$

$$u_n = -\frac{1}{\rho a^2}\left[\frac{\left(\omega + \overline{U}_n k_{1n}\right)}{k_{1n}} A_n e^{ik_{1n}X_n} + \frac{\left(\omega + \overline{U}_n k_{2n}\right)}{k_{2n}} B_n e^{ik_{2n}X_n}\right] e^{i\omega t} \tag{2.5}$$

where harmonic time dependence of the form $e^{i\omega t}$ has been assumed. The wave numbers k_{1n} and k_{2n} are the two complex roots of the equation

$$k_n^{\,2} + i\frac{f_n\left|\overline{U}_n\right|}{D_n a^2}\left(\omega + \overline{U}_n k_n\right) - \frac{1}{a^2}\left(\omega + \overline{U}_n k_n\right)^2 = 0 \tag{2.6}$$

where f_n is the pipe friction factor for element n and D_n is the hydrodynamic diameter for element n. A_n and B_n are complex constants which are a function of frequency and are determined by satisfying continuity of pressure and mass conservation at element junctions.

2.3 Low Frequency Contribution

[[

(3)]]

2.4 Modeling Parameters

When the steam dryer geometry is defined and the physical parameters at the power level of interest are provided (such as the mean steam flow in the main steam lines), the Helmholtz and acoustic circuit analyses are driven by seven modeling parameters: (1) the damping in the steam dome, (2) the proportionality constant in Equation (2.3) at the steam-froth interface beneath the steam dryer, (3) the proportionality constant in Equation (2.3) at the steam-water interface between the dryer skirt and steam dome, (4) the damping in the main steam lines, (5) the main steam line friction factor, (6) [[(3)]], and (7) [[(3)]]

2.5 Model Assembly and Algorithm

[[

(3)]]

[[

(3)]]

[[

(3)]]

3. Quad Cities Unit 2 Instrumentation and Plant Data

Strain gage pairs were mounted at two locations on the main steam lines, upstream of the ERV standpipes, as summarized in Table 3.1. These data proved reliable throughout the QC2 startup. Pressure sensors were positioned at 27 locations inside and outside the dryer, and were designated P1 to P27. The locations of the transducers can be found in [10]. Sensor P19 appeared to fail during data acquisition but still provided credible information. The strain gage data were taken at 2000 samples/sec, while the pressure sensor data were taken at 2048 samples/sec, on a different recording system. Thus, the two data sets each included a channel for a trigger. In this way a common zero time could be established for the strain gage pairs and the pressure sensors, so as to eliminate any phasing differences. The sampling rate was sufficient, as the analysis was conducted to 250 Hz.

Table 3.1. Location of strain gage pairs on QC2 main steam lines [3]. SG locations are measured from the inside of the steam dome, down the centerline of the MSL.

Main Steam Line	Upper SG Location (ft)	Lower SG Location (ft)
A	9.5	41.0
B	9.5	41.3
C	9.5	41.3
D	9.5	41.0

Two sets of data are used in the ACM Rev. 4.1 analysis. The first set of data was taken at a power level of 790 MWe, test condition TC32B, at Original Licensed Thermal Power (OLTP) conditions, as summarized in Table 3.2. These data were recorded prior to installation of Acoustic Side Branches to the QC2 standpipes. Subsequent to this installation, a second set of data was taken during power ascension, at 156 MWe, test condition TC2, at 26.5% OLTP conditions, as also summarized in Table 3.2.

Table 3.2. Summary of the power levels examined with the current methodology.

Exelon Test Condition	Data Collection Date	Electric Power Level (MWe)	Thermal Power Level (MWt)	MSL Mach Number
TC32B (OLTP)	05/10/05	790	2493	0.105
TC2 (Low Power)	04/19/06	156	665	0.024

4. Low Frequency Hydrodynamic Load Contribution

[[

(3)]]

[[

[3]]]

Figure 4.1. Normalized PSD of entrance source strengths η' for QC2 data (790 MWe). The colors indicate the main steam line data plotted.

5. Noise Reduction in Measured Main Steam Line Data

[[

(3)]]

[[

(3)]]

[[

(3)]]

[[

(3)]]

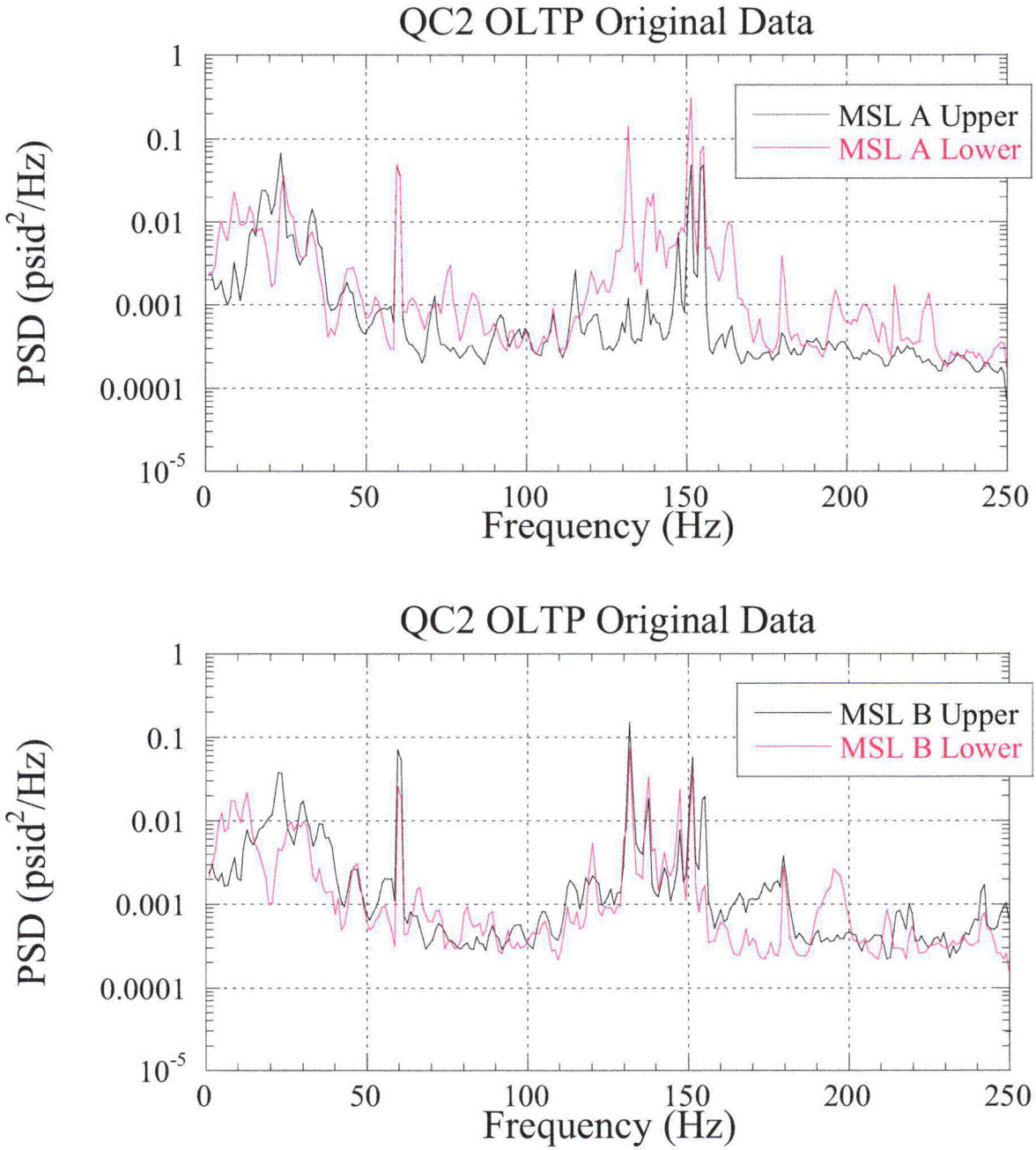

Figure 5.2a. PSD plots of the QC2 OLTP original data: MSL A (top), MSL B (bottom).

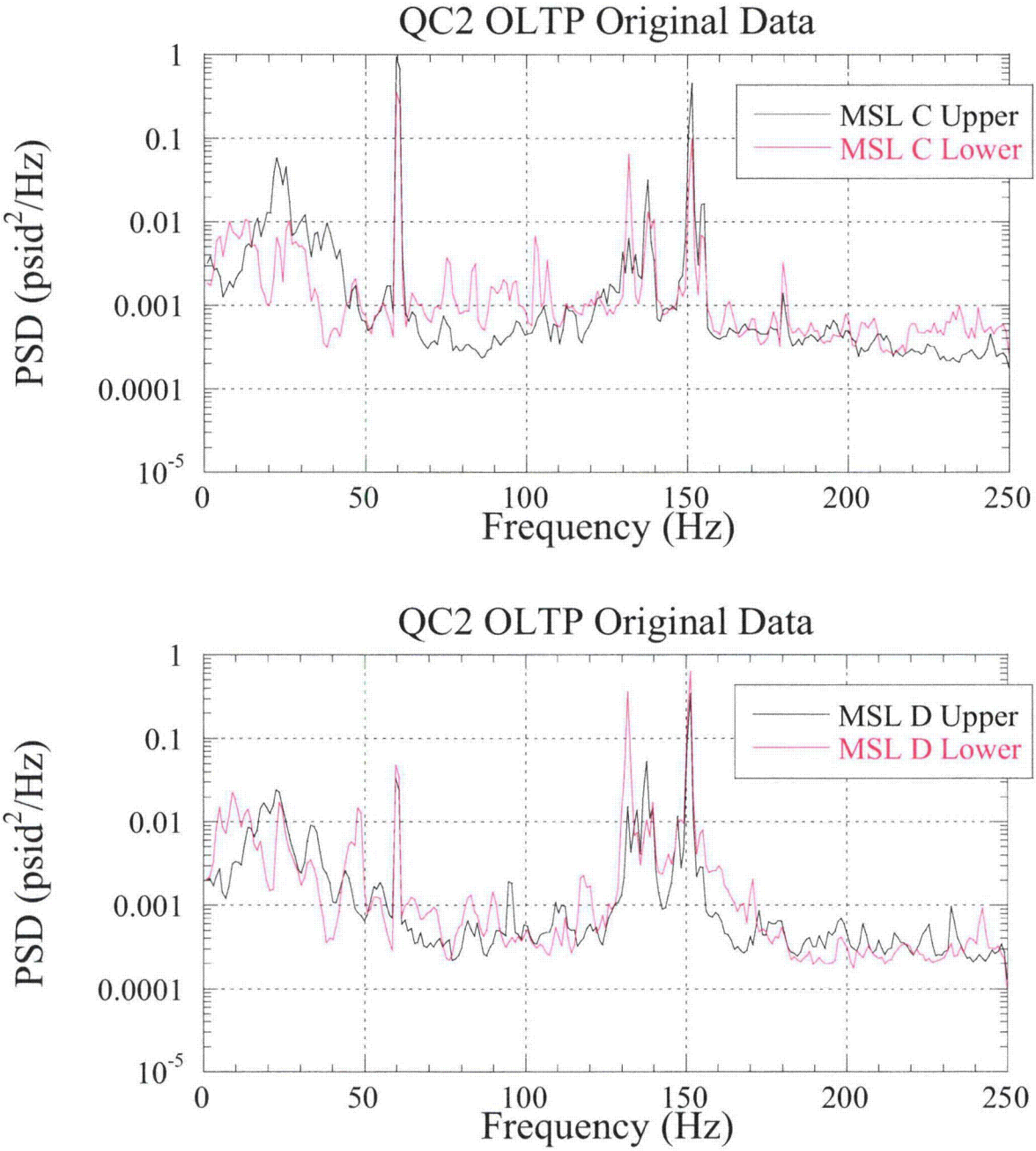

Figure 5.2b. PSD plots of the QC2 OLTP original data: MSL C (top), MSL D (bottom).

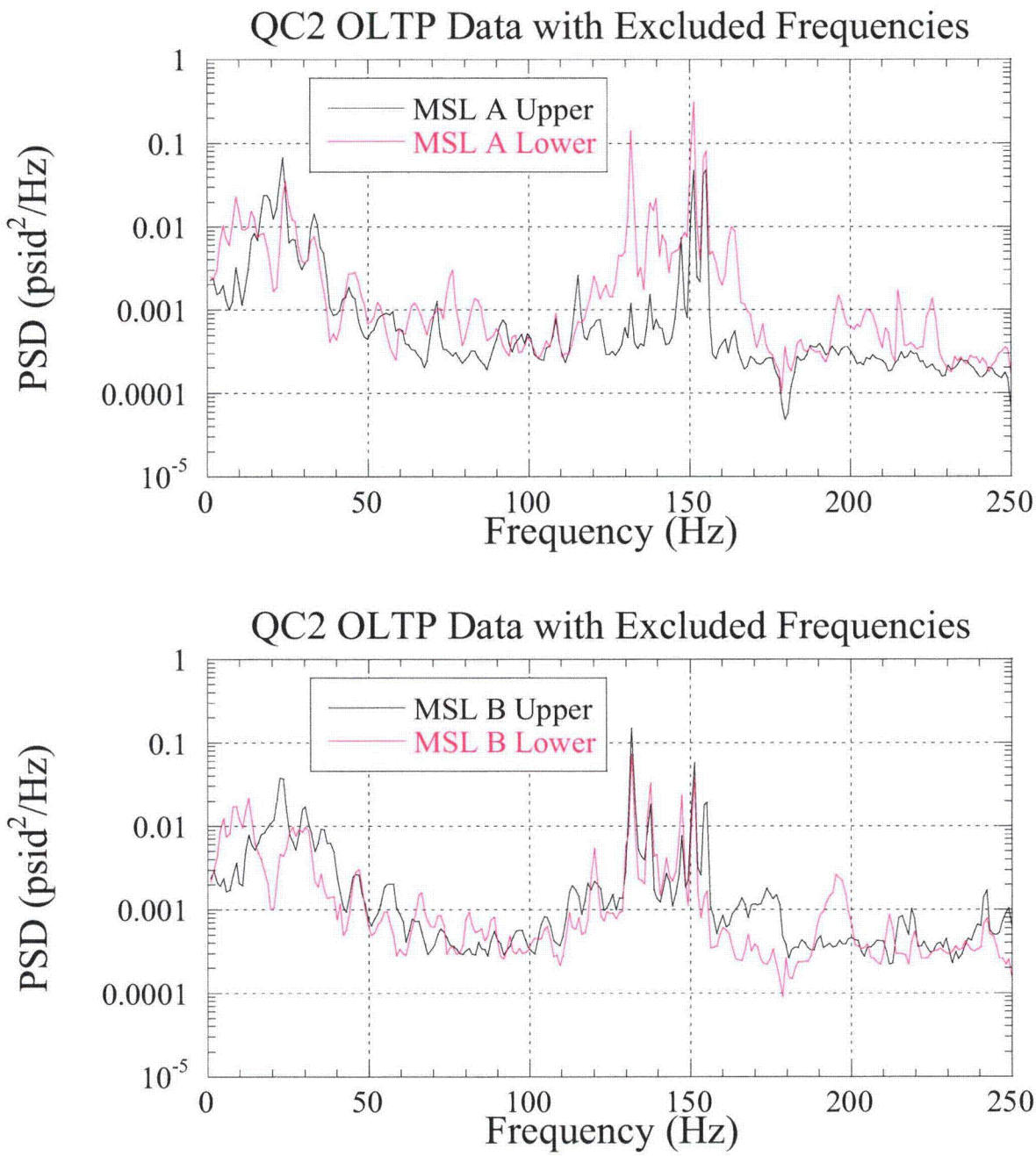

Figure 5.3a. PSD plots of the QC2 OLTP data with exclusion frequencies removed: MSL A (top), MSL B (bottom).

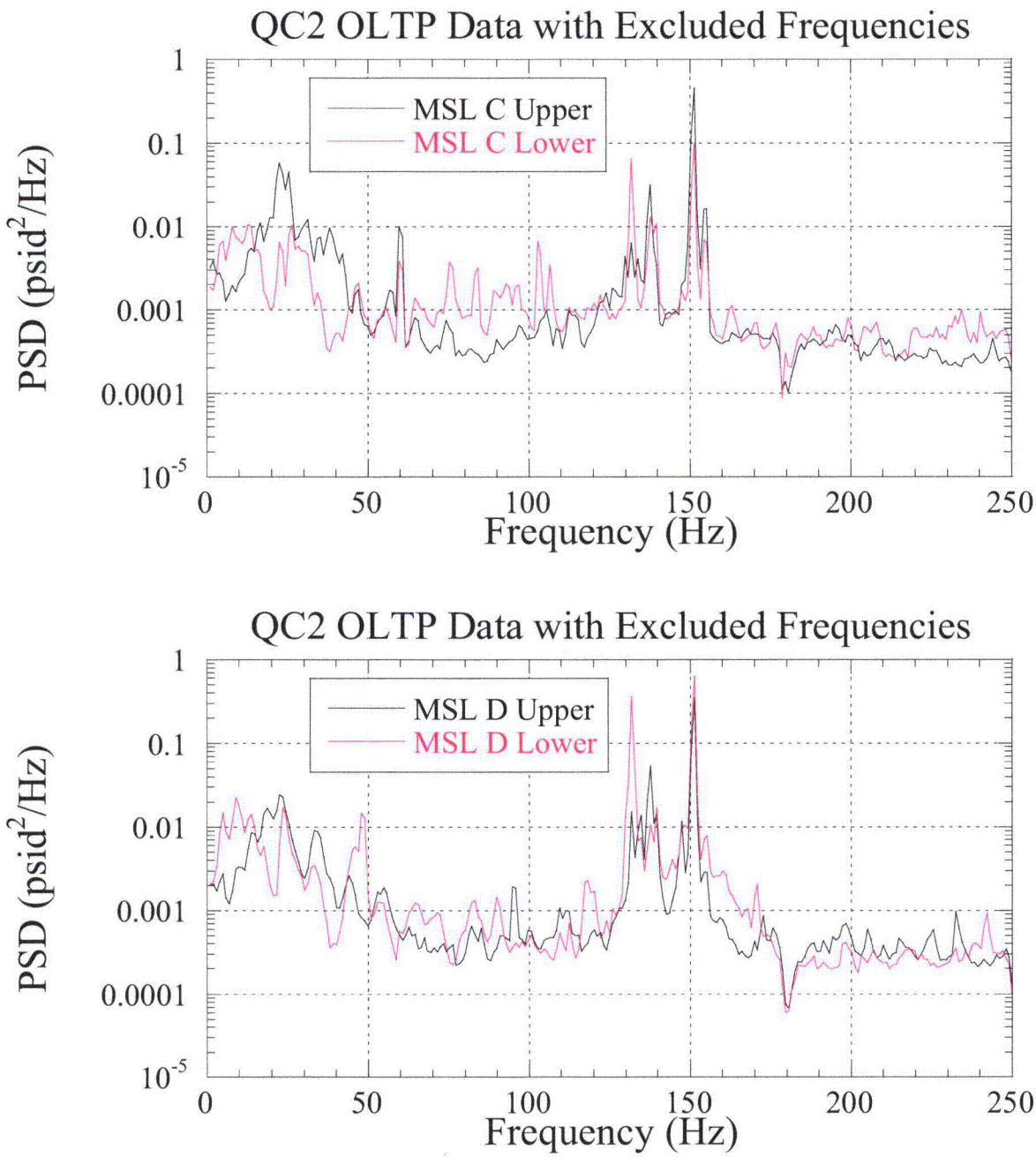

Figure 5.3b. PSD plots of the QC2 OLTP data with exclusion frequencies removed: MSL C (top), MSL D (bottom).

[[

[(3)]]

Figure 5.4a. Plots of the QC2 OLTP coherence factors γ_1 and γ_2, for MSL A (top) and MSL B (bottom). The upper factor is γ_1; the lower factor is γ_2.

[[

[(3)]]

Figure 5.4b. Plots of the QC2 OLTP coherence factors γ_1 and γ_2, for MSL C (top) and MSL D (bottom). The upper factor is γ_1; the lower factor is γ_2.

[[

[3]]]

Figure 5.5a. PSD plots of the QC2 OLTP data with coherence filtering applied: MSL A (top), MSL B (bottom).

[[

(3)]]

Figure 5.5b. PSD plots of the QC2 OLTP data with coherence filtering applied: MSL C (top), MSL D (bottom).

6. Model Predictions and Comparisons

Previous model evaluation predictions [3–6] provided several comparisons with pressure sensor data at the QC2 dryer sensor locations, for acceptance criteria first suggested by Exelon and later refined by C.D.I. The model parameters used in these studies are summarized in [6]. The prior development of the Modified Bounding Pressure model was necessitated by two conditions: [[

(3)]]

[[

(3)]]

Figure 6.1. ACM Rev. 4.1 pressure predictions at 790 MWe at the dryer pressure sensors: peak minimum (top) and peak maximum (bottom) pressure levels, with data (black) and predictions (red). Sensors P13, P14, P16, P23, and P27 are inside the dryer, while P26 is on a mast above the dryer.

[[

(3)]]

Figure 6.2a. PSD comparison at 790 MWe for pressure sensor data (black curves) and ACM Rev. 4.1 prediction (red curves), for P1 (top) and P2 (bottom).

[[

(3)]]

Figure 6.2b. PSD comparison for 790 MWe for pressure sensor data (black curves) and ACM Rev. 4.1 prediction (red curves), for P3 (top) and P4 (bottom).

[[

(3)]]

Figure 6.2c. PSD comparison for 790 MWe for pressure sensor data (black curves) and ACM Rev. 4.1 prediction (red curves), for P5 (top) and P6 (bottom).

[[

(3)]]

Figure 6.2d. PSD comparison at 790 MWe for pressure sensor data (black curves) and ACM Rev. 4.1 prediction (red curves), for P7 (top) and P8 (bottom).

[[

[3]]]

Figure 6.2e. PSD comparison at 790 MWe for pressure sensor data (black curves) and ACM Rev. 4.1 prediction (red curves), for P9 (top) and P10 (bottom).

[[

(3)]]

Figure 6.2f. PSD comparison at 790 MWe for pressure sensor data (black curves) and ACM Rev. 4.1 prediction (red curves), for P11 (top) and P12 (bottom).

[[

(3)]]

Figure 6.2g. PSD comparison at 790 MWe for pressure sensor data (black curves) and ACM Rev. 4.1 prediction (red curves), for P18 (top) and P19 (bottom).

[[

(3)]]

Figure 6.2h. PSD comparison at 790 MWe for pressure sensor data (black curves) and ACM Rev. 4.1 prediction (red curves), for P20 (top) and P21 (bottom).

7. Model Uncertainty

[[

(3)]]

[[

(3)]]

8. Application to QC2 Steam Dryer

In this section the QC2 main steam line data will be used as an example of how to apply bias and uncertainty to a plant, and predict dryer loads.

[[

(3)]]

Table 8.1. Bias and uncertainty contributions to total uncertainty for QC2. Note that the Pressure Sensor Location Uncertainty is relative to the strain gage locations at QC2 and is therefore zero in this example.

[[

(3)]]

Table 8.2. QC2 total uncertainty totals for specified frequency intervals.

[[

(3)]]

[[

(3)]]

Figure 8.1. Plots of the QC2 OLTP coherence, for MSL A and B (top), and MSL C and D (bottom).

[[

(3)]]

Figure 8.2a. PSD plots of the QC2 OLTP data with noise floor: MSL A (top), MSL B (bottom).

[[

(3)]]

Figure 8.2b. PSD plots of the QC2 OLTP data with noise floor: MSL C (top), MSL D (bottom).

[[

(3)]]

Figure 8.3. Predicted loads at the 27 sensor locations on the QC2 dryer, as developed by ACM Rev. 4.1 with bias and uncertainty included: peak minimum (top) and peak maximum (bottom) pressure levels, with data (black) and predictions (red). Sensors P13, P14, P16, P23, and P27 are inside the dryer, while P26 is on a mast above the dryer.

[[

(3)]]

Figure 8.4. PSD of the loads predicted on the A-B side of the QC2 dryer (pressure sensor P12, top) and the C-D side (pressure sensor P21, bottom), in red, compared to the OLTP data, in black. ACM Rev. 4.1 model predictions have been multiplied by the total uncertainty from Table 8.2, except at those frequencies where the noise floor is imposed.

9. Conclusions

The model evaluation examined here demonstrates the applicability of the C.D.I. acoustic circuit analysis for use with in-plant pressure data collected on the main steam lines. The model will be used with other steam dryer geometries and other main steam line configurations to provide a conservative and representative pressure loading on the steam dryer.

Instrumenting the main steam lines at optimum locations (discussed in [6]) would minimize uncertainty with regard to instrument placement along the main steam lines. Since the Helmholtz solution is geometrically unique, for each steam dome / dryer geometry, differences between plants are accounted for in the analysis. It is anticipated that the high quality of steam exiting the dryer and entering the main steam lines is similar between plants; thus, model parameter values should not be plant-dependent.

The results of this evaluation illustrate the following:

1. [[

   (3)]]

2. The model accurately predicts the PSD peak amplitude and frequency for all pressure sensors.

3. ACM Rev. 4.1 can be used for all plants that have main steam line Mach numbers comparable to the QC2 plant at OLTP conditions.

10. References

1. Continuum Dynamics, Inc. 2005. Quad Cities 2 New Dryer Vulnerability Loads. C.D.I. Technical Note No. 05-03.

2. Continuum Dynamics, Inc. 2005. Quad Cities 2 New Dryer SMT Loads. C.D.I. Technical Note No. 05-04.

3. Continuum Dynamics, Inc. 2005. Evaluation of Continuum Dynamics, Inc. Steam Dryer Load Methodology against Quad Cities Unit 2 In-Plant Data. C.D.I. Report No. 05-10.

4. Continuum Dynamics, Inc. 2005. Blind Evaluation of Continuum Dynamics, Inc. Steam Dryer Load Methodology against Quad Cities Unit 2 In-Plant Data at 2831 MWe. C.D.I. Technical Note No. 05-37.

5. Continuum Dynamics, Inc. 2005. Improved Methodology to Predict Full Scale Steam Dryer Loads from In-Plant Measurements. C.D.I. Report No. 05-23.

6. Continuum Dynamics, Inc. 2007. Bounding Methodology to Predict Full Scale Steam Dryer Loads from In-Plant Measurements (Rev. 3). C.D.I. Report No. 05-28 (Proprietary).

7. Continuum Dynamics, Inc. 2007. Methodology to Predict Full Scale Steam Dryer Loads from In-Plant Measurements, with the Inclusion of a Low Frequency Hydrodynamic Contribution (Rev. 1). C.D.I. Report No. 07-09 (Proprietary).

8. NRC Request for Additional Information on the Hope Creek Generating Station, Extended Power Uprate. 2007. RAI No. 14.11.

9. Continuum Dynamics, Inc. 2005. Methodology to Determine Unsteady Pressure Loading on Components in Reactor Steam Domes (Rev. 6). C.D.I. Report No. 04-09 (Proprietary).

10. General Electric Company (C. Hinds). 2005. Dryer Sensor Locations. Letter Report No. GE-ENG-DRY-087. Dated 18 May 2005.

11. Structural Integrity Associates, Inc. 2008. Nine Mile Point Unit 2 Strain Gage Uncertainty Evaluation and Pressure Conversion Factors (Rev. 1). SIA Calculation Package No. NMP-26Q-301.

12. J. S. Bendat and A. G. Piersol. 1966. Measurement and Analysis of Random Data. John Wiley and Sons. See page 215, Table 5.1.

13. Communication from Enrico Betti. 2006. Excerpts from Entergy Calculation VYC-3001 (Rev. 3), EPU Steam Dryer Acceptance Criteria, Attachment I: VYNPS Steam Dryer Load Uncertainty (Proprietary).

14. Exelon Nuclear Generating LLC. 2005. An Assessment of the Effects of Uncertainty in the Application of Acoustic Circuit Model Predictions to the Calculation of Stresses in the Replacement Quad Cities Units 1 and 2 Steam Dryers (Revision 0). Document No. AM-21005-008.